Forensic Science International 229 (2013) 163.e1–163.e6

Contents lists available at SciVerse ScienceDirect

Forensic Science International

journal homepage: www.elsevier.com/locate/forsciint

Forensic Anthropology Population Data

Estimating postmortem interval using RNA degradation and morphological changes in tooth pulp

Stephanie T. Young [a], Jeffrey D. Wells [a,b], Gerald R. Hobbs [c], Clifton P. Bishop [a,*]

[a] Department of Biology, West Virginia University, 53 Campus Drive, Morgantown, WV 26506, USA
[b] Department of Biological Sciences, Florida International University, 1120 SW 8th Street, Miami, FL 33199, USA
[c] Department of Statistics, West Virginia University, P.O. Box 6330, Morgantown, WV, USA

ARTICLE INFO

Article history:
Received 7 December 2011
Received in revised form 2 January 2013
Accepted 20 March 2013
Available online 4 May 2013

Keywords:
Postmortem interval
Ribonucleic acids
Quantitative reverse transcription real-time polymerase chain reaction

ABSTRACT

The accurate determination of time since death, or postmortem interval (PMI), can be critical in the investigation of suspicious deaths. Knowing when a suspicious death occurred can limit the number of potential suspects to those without a viable alibi for the time of the crime. The forensic techniques currently employed to determine PMI: pathology, entomology, and anthropology, are accurate over different time periods following death. A large gap in time exists between the capabilities of forensic entomology and traditional anthropology, leaving a period in which PMI is difficult to estimate. In this study, time-dependent differences in RNA decay rates were examined to extend the time frame over which early PMI estimates can be made. Comparing the decay rates of a large, labile segment of β-actin RNA and a smaller, more stable, non-overlapping segment of the same RNA from tooth pulp, we were able to estimate PMI values of pigs buried within a shallow grave for up to 84 days. This compares favorably to an estimate of PMI using insect data. Full skeletonization and loss of insect activity was observed by day 28 of our study. In addition to differences in RNA decay rates, morphological changes were observed in the pulp as it aged postmortem. To provide a quantitative measure of progressive color changes, analysis of digital photographs of each tooth's pulp were used to construct a simple colorimetric assay. This assay was then used to cluster ages of pulp samples by color. The two assays, used in combination with one another, can create a more precise estimate of PMI. The potential advantages of this molecular means of estimating PMI include extending the time frame for such estimates, is applicable to samples collected worldwide (no specialized knowledge of local insect fauna is required), is relatively fast, and inexpensive.

1. Introduction

Estimation of postmortem interval (PMI), or time since death, is a common component of a death investigation. Knowing PMI helps investigators reconstruct the circumstances in the case of a suspicious death or homicide and can limit the number of potential suspects by excluding those with viable alibis for the time of the crime.

Modern techniques in the estimation of PMI rely mainly upon predictable, histochemical changes that occur within the body following death or the temperature-dependent development and succession of corpse-colonizing insects. These techniques can be divided into methods that are pathological, entomological, or anthropological, with each having a length of time following death in which they are most useful. In predicting early (hours to days) to extended (years) PMIs, the order of methods employed usually follows as: pathology, entomology, and finally anthropology. Each method occupies a niche in the time line between death and body discovery, with a pronounced gap between the capabilities of forensic entomology and anthropology.

Pathological methods [1–6] employ fluctuating variables which predominately occur within a four-day period postmortem, after which these methods can no longer provide an accurate estimate of PMI. To determine PMIs that are longer than roughly four days, investigators currently rely upon forensically significant insect species to formulate early estimates, while anthropology can provide information to estimate greatly extended PMIs.

Forensic entomology utilizes the PMI-dependent processes of carrion insect development and/or species succession [7]. These phenomena are a function of environmental conditions, which must be well-understood to make a precise and accurate PMI estimate. Although there are several forensically significant insect

* Corresponding author. Tel.: +1 304 293 5245; fax: +1 304 293 6363.
E-mail address: cbishop@mail.wvu.edu (C.P. Bishop).

0379-0738/$ – see front matter © 2013 Elsevier Ireland Ltd. All rights reserved.
http://dx.doi.org/10.1016/j.forsciint.2013.03.035

orders, the carrion flies of order Diptera are most often used for PMI estimation due to their rapid colonization of a corpse following death [8]. The most precise estimates of maggot age (having smallest confidence intervals) occur during periods of rapid change in variables such as larval length and/or weight [7]. Although all developmental stages of dipterans can be used in an entomological estimate of PMI, few abrupt changes occur during postfeeding stages [7]. Thus, the most powerful estimates using Diptera are usually made while there is soft tissue, the larval food source, remaining on the corpse. At skeletonization, soft tissues have either decomposed or have been completely consumed. Any remaining individuals in immature stages will either move on to find another food source in close proximity, go into stress–response pupariation [9], or perish. The technique is also limited by a multitude of environmental and situational variables (similar to those that affect tissue decomposition), such as whether the corpse is in direct sunlight or in shade, above ground or buried below ground, and the amount of clothing the individual may have been wearing at the time of fatality [10]. Insects must have access to the corpse, which becomes more difficult for certain species in the cases of burial or other means of entombment. There is a need for expert knowledge of local insect fauna, and the developmental data for these insects at different temperatures must be known (which can make the technique geographically restricting).

Forensic anthropology can also be used in the estimation of extended PMIs of years to centuries in length. It can be difficult in the case of skeletal remains, however, to provide more information than whether a bone is recent, old, or archeological [11].

Other research groups have also seen the need to expand the timeframe in which early estimates of PMI can be made. These attempts include changes in element composition in soil under bodies [12], changes in ninhydrin reactive hydrogen in soil [13], and changes in microbial-derived ATP [14]. Although these methods have potential, the large amount of variation in their data renders PMI estimates of limited value.

The goal of this study was to provide a universal method of PMI estimation that can surpass the amount of time following death in which estimates can currently be made with the use of pathology and/or entomology. In order to accomplish this, we have applied a variation of our previous molecular-based method for estimating the age of a dried bloodstain [15,16] to estimate the PMI of a corpse buried in a clandestine, shallow grave. This approach has also been used by Hampson et al. [17] to estimate the *ex vivo* age of hair follicles. In a process somewhat analogous to carbon-14 dating, where the ratio of radioactive carbon to non-radioactive carbon changes over time (due to radioactive decay of ^{14}C) [18], the disappearance of a less stable molecule relative to that of a more stable molecule can be used to estimate PMI. In the past, we have used quantitative real-time PCR (qPCR) to demonstrate that differently sized segments of ribonucleic acids (RNAs) degrade at different rates in *ex vivo* blood samples [16], and as presented here, in postmortem tooth pulp. Longer RNAs degrade more rapidly than do shorter RNAs merely due to a function of their size. A larger RNA target has a higher probability of intercepting insults from the environment than does a small target. The differential rates of decay can be used to calculate PMI.

Other labs have also examined changes in RNA as a means to estimate PMI. Inoue et al. [19] examined mRNA degradation profiles in dead rat brain, lung, heart, and liver over a seven-day time period. Bauer et al. [20] examined RNA from stored blood and brain samples aged between 7 and 145 h postmortem. While Zhao et al. [21] looked at degradation profiles for three genes from forensic autopsy material from heart, brain, kidney, and lung samples over a time period of 0–72 h. All of these studies were conducted over a relatively short time frame involving samples from soft tissues and showed highly variable results. In contrast, we conducted a study of extended PMI using tooth pulp.

Tooth pulp was chosen for study due to the morphology of mammalian teeth. Held within the protective outer enamel of the tooth is found a soft tissue, tooth pulp, rich in genetic material. We suspected that tooth pulp, when compared to other types of tissue, is more protected from external elements such as high humidity, exposure to direct sunlight, wet weather conditions, bacterial infestation, and potential insect or terrestrial scavengers. We have also developed a simple, but novel, approach to quantitatively measure changes in tissue coloration as it decays. Changes in pulp appearance have been observed by other groups as well. In 1991, Duffy et al. [22] reported a subjective means of estimating PMI based upon visual pulp putrification. In 2010, Menon et al. [23] looked at histological changes in dentin, cement, and pulp from extracted teeth and concluded it was not possible to infer the elapsed period of burial by their approach. Our colorimetric assay alone is not sufficient to produce a precise estimate of PMI, but when used in conjunction with the RNA analysis, provides a more accurate measure of PMI.

2. Methods

2.1. Burial technique and sample collection

Eight pig heads were obtained from a local meat market, Emerick Meat & Packing (Hyndman, PA). The heads were transported to the West Virginia University Plant and Soil Sciences Farm where they were buried in a shaded area approximately 7.5 cm below the ground's surface in a shallow grave. The total elapsed time from death until burial and day 0 tooth extraction was less than 6 h. Chicken wire was placed over the top of each grave and secured with tent pegs to exclude scavengers. Two teeth were randomly sampled from each pig on days 0, 7, 14, 21, 28, 42, 56, 70, 84, 98, 112, 126, and 140. Teeth that were determined visually to be severely diseased were not collected for study.

2.2. RNA extraction from tooth pulp

All teeth were transported to a laboratory and processed within 2 h of extraction. The surface of each tooth was washed with cool water and antibacterial soap. The cleaned tooth was placed in a ceramic mortar, frozen with liquid nitrogen, and struck with a pestle to expose the pulp. RNA was extracted from small sections of tooth pulp using a mono-phase solution containing both phenol and guanidine thiocyanate, TRI-Reagent RT (Molecular Research Center, Cincinnati, OH). The pulp from each tooth was ground in a glass tissue grinder in the presence of 350 μl TRI-Reagent RT until no large pieces of pulp remained. The homogenate was transferred to a 1.5 ml tube containing 650 μl of TRI-Reagent RT. After mixing by vortex, the samples were incubated at room temperature for 5 min. Centrifugation followed for 10 min. All centrifugations were performed at 12,000 × *g* at 4 °C. Approximately 950 μl of supernatant was decanted and placed into a new 1.5 ml tube. To each sample, 175 μl 1-bromo-3-chloropropane (Molecular Research Center) was added and the samples briefly mixed using a vortex. After centrifugation for 15 min, the aqueous phase of the samples was removed and placed in a new 1.5 ml tube. To each sample, 500 μl of cold isopropanol was added and the tubes inverted to mix. After room temperature incubation for 8 min, the samples were centrifuged for 5 min. The supernatant was removed and 1 ml of 75% ethanol was used to wash the remaining RNA pellet. The samples were again centrifuged for 5 min. The ethanol was decanted and the pellet air-dried in a fume hood for 5 min. To resuspend the pellet, 40 μl nuclease-free water (Fisher Scientific, Pittsburgh, PA) was added and the sample was heated for 10 min at 55 °C.

2.3. qPCR screen for genomic DNA contamination

All custom designed primer and probe combinations for real-time PCR were designed using Primer Express software version 3.0 and synthesized by Applied Biosystems (Foster City, CA). Primer and probe sequences can be found in Table 1. DNA-specific primers and probes were designed to detect the presence of a non-transcribed portion of the porcine glyceraldehyde-3-phosphate dehydrogenase (GAPDH) gene. This screen indicates whether or not DNA contamination was present in our RNA isolates. Two sets of primers/probes were created to amplify a 71 base pair and a separate 83 base pair region of the GAPDH gene. These amplicons were designated PGAP71 and PGAP83, respectively. Two sets of primers/probes were used in case of polymorphism in the primer or probe binding sites of the GAPDH gene of subjects. RNA samples (5 μl) were run in a multiplex real-time PCR reaction with each of the previously mentioned primer/probe combinations in a PCR master mix having a final concentration of: 200 nM PGAP71 forward and reverse primer, 250 nM PGAP71 VIC-labeled probe, 500 nM PGAP83 forward and

Table 1
Real-time PCR primers and probes used to amplify porcine β-actin mRNA and GAPDH DNA.

Name	Size amplified (bp)	Specificity	Primer/probe sequence
PGAP71	71	DNA-specific	FP: 5′-GGCTGACTTGGACCAGGAAAG-3′ RP: 5′-CCCTTCAAGTGAGCCTGCAG-3′ Probe (VIC): 5′-AAGCCCGGGTGTCTGACTGCTCC-3′
PGAP83	83	DNA-specific	FP: 5′-AAGTATGGAAGACGGAACCGG-3′ RP: 5′-GGGACCACAGACCCAAGGT-3′ Probe (FAM): 5′-AGGAGGTGGTGCTGGGACGGG-3′
PBA71	71	RNA-specific	FP: 5′-TCGCCGCCGGTCTACA-3′ RP: 5′-GCCGTTGTCGACCACGAG-3′ Probe (VIC): 5′-CGCCATGGATGACGATATTGCTGC-3′
PBA301	301	RNA-specific	FP: 5′-ACCGACTACCTCATGAAGATCCTG-3′ RP: 5′-GCACTTCATGATGGAGTTGAAGG-3′ Probe (FAM): 5′-CTGCCCGACGGCCAGGTCATC-3′

reverse primer, 250 nM PGAP83 FAM-labeled probe, 12.5 μl of Applied Biosystems Universal PCR Master Mix (a pre-mixed solution containing AmpliTaq Gold DNA polymerase, dNTPs, a passive reference, and proprietary buffers for stabilization), and nuclease-free water to bring the final volume of the mix to 20 μl. The real-time PCR reaction for each sample was run using an Applied Biosystems Prism 7300 Sequence Detection System under default conditions (1 cycle 50 °C for 2 min, 1 cycle 95 °C for 10 min, and 40 cycles alternating between 95 °C for 15 s and 60 °C for 1 min). A positive control was included in each run that contained 20 μl master mix and 5 μl porcine DNA (550 ng/ul). Two negative controls were also included: the first being 20 μl master mix and 5 μl nuclease-free water, and the second, 25 μl nuclease-free water. Amplification resulting in Ct values below 35 in our RNA isolates is indicative of residual DNA contamination [24,25].

2.4. Reverse transcription

RNA samples were reverse transcribed to cDNA with an Applied Biosystems' Taqman Gold Reverse RT-PCR kit. A reverse transcription mix was created with final concentrations: 1× Taqman buffer A, 2.5 μM random hexamers, 5.5 mM magnesium chloride, and 500 μM each dATP, dCTP, dGTP, and dTTP. 57 μl of the reverse transcription mix was combined with 40 μl of RNA isolate, 2 μl of RNase inhibitor (0.8 U), and 2.5 μl of Multiscribe reverse transcriptase (3.25 U). The samples were then pulse centrifuged, placed into a Techne Touchgene Gradient thermocycler (Burlington, NJ), and run under the following conditions: 25 °C for 10 min, 48 °C for 30 min, 95 °C for 5 min.

2.5. qPCR quantification of RNA

Two sets of porcine-specific, RNA-specific primers and probes were created in order to amplify two separate, non-overlapping regions within β-actin messenger RNA (mRNA). One set of primers, designated PBA71, amplifies a 71 base pair segment, while the other, PBA301, amplifies a 301 base pair segment of the same mRNA molecule. Primer and probe sequences can be found in Table 1. The multiplex reaction was tested for efficiency using the guidelines and recommendations of Livak and Schmittgen [26]. Each cDNA sample (5 μl) was run in multiplex with final master mix concentrations of: 100 nM PBA71 forward and reverse primer, 250 nM PBA71 VIC-labeled probe, 1100 nM PBA301 forward and reverse primer, 250 nM PBA301 FAM-labeled probe, 12.5 μl of Applied Biosystems Universal PCR Master Mix, and nuclease-free water to bring the final volume of the mix to 20 μl. The real-time PCR reaction for each sample was run in duplicate using an Applied Biosystems Prism 7300 Sequence Detection System under the following conditions: 1 cycle 50 °C for 2 min, 1 cycle 95 °C for 10 min, and 40 cycles alternating between 95 °C for 15 s and 60 °C for 3 min. A positive control was included in each run that contained 20 μl master mix and 5 μl porcine cDNA (525 ng/ul). Two negative controls were also included: 20 μl master mix and 5 μl nuclease-free water, as well as a second control of 25 μl nuclease-free water.

2.6. qPCR data analysis

Cycle threshold (Ct) values were obtained by setting the real-time PCR baselines and thresholds according to Applied Biosystems' recommendations. These values were kept constant for all real-time PCR applications. Once Ct values were obtained for all samples, the data were imported into Microsoft Excel (Microsoft Corporation, Redman, WA). Because Ct values of 35 or higher indicate 1–0 copies of the target RNA present in a sample [24,25], any sample producing a Ct value of 35 or higher was removed from further analysis. Duplicate samples where raw Ct values differed more than 0.5, *i.e.* greater than reported for machine error, were thought to represent operator/pipette error such as a mis-loaded sample. These were also removed from further analysis. All remaining Ct values were transformed using the $2^{-\Delta Ct}$ data conversion of Livak and Schmittgen [26]. This conversion is necessitated by the fact that the Ct values are measured on a logarithmic scale. The ΔCt portion of the conversion was calculated by subtracting the Ct value of the 71 bp region from the 301 bp region for all samples.

2.7. Colorimetric analysis

Each tooth, once broken open, was photographed using a Leica MZ16 high-performance stereomicroscope and supporting Leica FireCam software version 1.9.1 (Bannockburn, IL). Parameters for each photo were as follows: exposure at 127 ms, gain at 3.1×, and saturation at 121%.

The color of exposed tooth pulp within the photos was analyzed using Adobe Photoshop version 7.0 (Adobe Systems Incorporated, San Jose, CA) RGB mode. A standard for the colors red, green, and blue was photographed adjacent to each tooth to later normalize for indoor light intensity variation. Along with the 3 color standards, 3 points (pixels) were randomly selected on the exposed pulp in each photograph and color intensity values were recorded for the colors red (R), green (G), and blue (B). Pure red, green, or blue coloration of a pixel in Photoshop has an intensity value of 255 for its respective color while producing an intensity value of 0 for all others [27]. For example, the intensity values for pure red are R: 255, B:0, and G:0. Each photograph was corrected for each color standard's deviation from pure red, green, and blue in order to standardize all photos.

Correction factors were determined by first calculating each color standard's deviation from pure red, green, or blue. For example, the standard for red (RS) in one photograph will yield three observed intensity values, one for red (RS_R), green (RS_G), and blue (RS_B), respectively. To determine the red correction factors (RCFs), each color must be taken into consideration:

$$RCF_R = 255 - RS_R$$

$$RCF_G = 0 - RS_G$$

$$RCF_B = 0 - RS_B$$

The correction factors for green and blue were calculated in a similar manner where the standard being examined was always subtracted from 255 (intensity value for pure coloration) while others are subtracted from 0.

To obtain a corrected estimate of red coloration of a sample ($Sample_R$), the correction factors were added to the observed intensity value recorded for red (R_{obs}):

$$Sample_R = R_{obs} + RCF_R + RCF_G + RCFB$$

This equation was repeated for both observed green and blue coloration in each sample. Samples used for RNA degradation analyses were excluded from color analysis if no pulp remained to be photographed after RNA isolation procedures. The average values for each color, for each tooth, were analyzed using k-means cluster analysis ($k = 3$). Cluster analysis was performed using JMP version 8 (SAS Institute Inc., Carry, N.C.) in order to determine statistical similarities in color between samples with varying PMIs.

3. Results

3.1. Multiplex qPCR primer/probe efficiency

An assumption of the $2^{-\Delta Ct}$ method [26] of qPCR analysis is that the efficiencies of the two primer/probe combinations (PBA301 and PBA71) are comparatively equal to one another in a multiplex reaction (one is not being preferentially amplified over another). Therefore, in order to obtain accurate results from qPCR using this method, the efficiencies of the amplicons in multiplex were

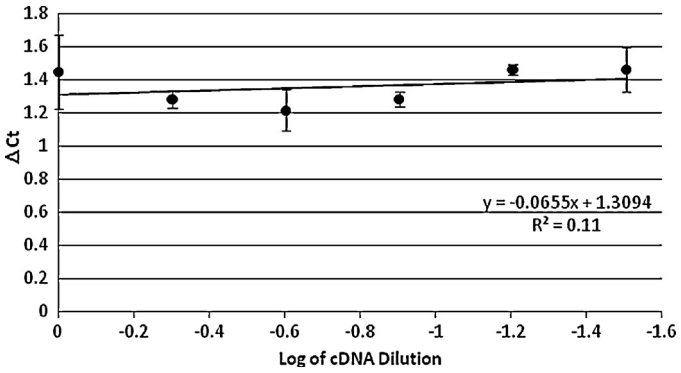

Fig. 1. Multiplex qPCR efficiency. To determine efficiency of the primer/probe multiplex combination of PBA301 and PBA71, the log of serial cDNA dilutions was plotted against the ΔCt ($Ct_{PBA301} - Ct_{PBA71}$). The absolute value of the slope determines the efficiency of amplification of each primer/probe combination during a multiplex real-time reaction. Bars represent standard errors where $n = 36$ duplicate samples of varying dilutions.

validated (slope = −0.0655) (Fig. 1). Efficiency increases as the absolute value of the slope reaches zero.

3.2. Analysis of genomic DNA within RNA samples

Amplification of all tooth pulp extracts using primers/probes for porcine GAPDH genomic DNA contamination yielded Ct values greater than 35 (results not shown). Therefore, all isolated RNA samples were deemed clear of DNA and ready for downstream reverse transcription and subsequent real-time PCR applications.

3.3. Postmortem pulp RNA degradation

RNA degradation was determined with the use of qPCR. The Ct values obtained from each sample were analyzed using the data conversion $2^{-\Delta Ct}$ (Fig. 2). The higher the value of $2^{-\Delta Ct}$ generated from a sample, the greater the similarity in the concentration of the small and the large β-actin amplicons. Decreases in this value with increasing PMI reflect differential degradation, in which the large portion of the RNA molecule is found in lower quantities than the smaller, more stable portion of the molecule.

Fig. 2 illustrates how the 301 bp segment of β-actin mRNA degraded more rapidly than the 71 bp portion. This trend continued until a PMI of 84 days, at which point the larger fragment could no longer be detected. Therefore, under the conditions of this experiment, our RNA method cannot determine an estimate of PMI beyond this time period. The most precise estimations of PMI using this method will be gained from areas of Fig. 2 in which the decline of $2^{-\Delta Ct}$ is the most steep. Therefore, using this 301 bp and 71 bp segment of β-actin mRNA, there was seen reduced PMI resolution between days 14, 28, 42, and 56. This is noticeable in the flattened area of the figure.

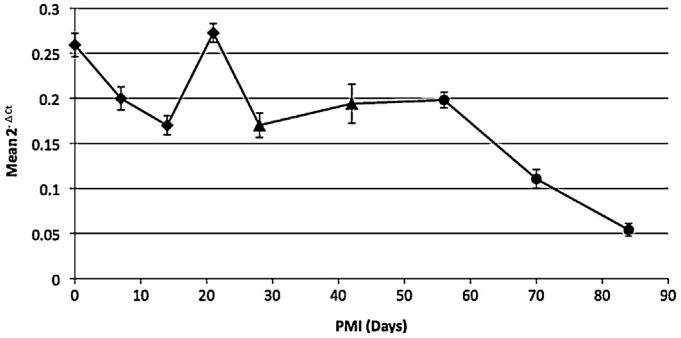

Fig. 2. RNA degradation within aging postmortem tooth pulp. Differential RNA degradation in tooth pulp over time as shown after statistical analysis using the $2^{-\Delta Ct}$ conversion. Depicted are the differences in degradation of a 301 bp and a 71 bp region of porcine β-actin mRNA extracted from postmortem tooth pulp over 84 days. Error bars represent standard error where $n = 192$ duplicate pulp samples. Each point is represented by one of three different shapes determining if that particular age was later assigned to cluster #1 (◆), cluster #2 (▲), or cluster #3 (●) during multivariate *k*-means cluster analysis of color.

Table 2
Mean color values for each cluster determined by *k*-means cluster analysis. Three pixels from the photograph for each aging tooth's pulp were analyzed for a numerical value of color using RGB mode in Adobe PhotoShop. The values for each color (red, green, or blue) were averaged together for each tooth. These values, after being subjected to multivariate cluster analysis using *k*-means led to the division of the data into three clusters of color. The mean and standard deviation (SD) of each cluster is presented where $n = 114$ teeth.

Cluster	Red	Green	Blue
1	243.696 (SD 9.044)	151.933 (SD 16.198)	120.993 (SD 25.321)
2	268.148 (SD 17.506)	245.049 (SD 19.391)	221.099 (SD 33.925)
3	236.841 (SD 16.919)	202.159 (SD 16.113)	156.841 (SD 30.093)

3.4. Colorimetric analysis of pulp decomposition

Morphological changes in the pulp as it aged were observed. Visual analysis of the pulp revealed four morphological stages similar to those described by Duffy et al. [22]. Some of these changes in pulp coloration and/or texture corresponded directly to the aforementioned interruptions and flattened areas seen in Fig. 2. In order to determine if a correlation existed between increasing PMI and morphological changes within the pulp as it aged, an analysis of aging pulp color was performed.

Using the RGB settings of Adobe Photoshop, a quantitative measure of color was obtained for red, green, and blue from three randomly selected pixels of each pulp image. The mean corrected color values for each tooth at varying ages postmortem was then subjected to *k*-means cluster analysis. Three clusters were found with means and standard deviations of each cluster presented in Table 2. Samples with an intermediate value of red, and low values of green and blue separated into cluster #1. Cluster #2 consisted of samples with high values for all color measurements. Finally, samples with low values of red and intermediate values of green and blue separated into cluster #3.

The ages of pulp samples that fell into each cluster based on color is shown in Table 3. Statistical analysis revealed that the majority (71%) of pulp samples from days 0, 7, 14, and 21 would be in cluster #1 having a higher red coloration with less green and blue. The next stage of visual decomposition, comprising cluster #2, began when pulp lost coloration and became pink-to-white.

Table 3
Contingency table – teeth by age sorted into clusters using multivariate *k*-means cluster analysis. After sorting tooth pulp samples into color clusters, the ages of the samples falling into each cluster was analyzed. The number of teeth from each age group (PMI) that fall into each of the three identified color clusters is presented. Underlined numbers are those samples correctly placed into a specific cluster.

Cluster	PMI								
	0	7	14	21	28	42	56	70	84
1	12	13	7	7	4	0	1	1	0
2	2	0	0	0	5	11	6	1	2
3	2	1	4	3	2	3	9	10	8
Total	16	14	11	10	11	14	16	12	10

Cluster #2 includes 78% of samples from days 28 to 42. At later stages of decomposition, pulp became more yellow to brown in coloration. This is shown in cluster #3, where the lowest values of red and blue are present. This final cluster included the majority of samples (64%) taken from pulp with a PMI of days 56, 70, and 84.

4. Discussion and conclusions

Although these results are based on a relatively small sample, the fact that both relative RNA degradation rates and color were a function of PMI until day 84 suggests that these measurements could be extremely valuable for estimating time since death. Because relative RNA degradation behaved in a non-linear fashion, use of tooth pulp RNA levels alone for PMI estimation would be complicated, but still possible. If Fig. 2 were considered to be an appropriate model for crime scene conditions, high values (approximately 0.26) of differential RNA degradation (calculated as $2^{-\Delta Ct}$) would suggest a PMI of about 25 days or less. Intermediate values (approximately 0.17–0.2) would indicate a PMI of about one week to 60 days. Although not entirely definitive of a precise PMI, samples resulting in these values could be used for exclusionary purposes. Because the curve is nearly linear with non-zero slope after day 56, a much more precise estimate of PMI is possible from about day 60 to day 84.

Further refinement of a PMI estimate is possible by also considering tissue color. Morphological changes in the pulp as it ages have been observed in the past [22,23]. We have provided a means of obtaining a quantitative, numerical value for color observation. These values can be analyzed in a short amount of time and can be used to partition the results of RNA degradation analysis (Fig. 2). For example, cluster #1 coloration was very rarely observed in teeth from 42 to 84 days (<5%). Therefore, a sample resulting in pulp coloration that falls within cluster #1 would support an age of no more than 42 days and would be consistent with intermediate RNA values placing the PMI between 7 and 60 days. Combined, these results would suggest a PMI of between 7 and not more than 42 days. In the color analysis, however, all samples of the same age were not always placed into the same color cluster, demonstrating that this type of colorimetric assay does not have sufficient power of discrimination to determine PMI on its own. The combination of the results from these two experimental variables (RNA degradation and colorimetric analysis) can be used together to produce a more precise estimate of PMI than either could provide alone. The 84 day interval during which mRNA levels and pulp color behaved as potential PMI indicators extended well beyond both the approximately four-day window for standard pathological PMI methods and the point at which the pig heads became skeletonized (day 28), *i.e.* the stage at which forensic insect activity significantly drops. The use of RNA degradation analysis, combined with numerical morphological measurements within tooth pulp in this study, tripled the amount of time in which a reliable estimate of PMI could be calculated.

The steady decline in our measurement of differential RNA degradation seen in Fig. 2 is interrupted by a peak at day 21. We observed the same phenomenon in previous unpublished studies using this particular set of primers and probes on RNA extracted from decaying tooth pulp. The raw data (not shown) indicates that this peak is due to a sudden increase in the degradation of the 71 bp amplicon while the degradation of the 301 bp amplicon slowed. The peak is therefore not due to an increase in undegraded β-actin mRNA. The presence of this peak, in both past and present studies, corresponded to a morphological transitional stage in the coloration and texture of the aging tooth pulp, which led to the pursuit of the colorimetric assay. Possible reasons for this anomalous data point include a change in the enzymes being released by the decomposing tissue or by other chemical products of degradation that were not present up until this point. An influx in bacterial load within the pulp could also play a role in RNA degradation at this point in time. Although there are no data at present to support these hypotheses, it is of interest to pursue in future studies. The presence of this peak marks a length of time (between days 14 and 28) in which a precise estimate of PMI using these specific primers and probes may be more difficult to calculate. With future analysis of the degradation of different types and sizes of RNAs, along with the pulp color analysis presented here, the authors hope to provide better resolution in the estimates of PMI.

The levels of any given RNA species can vary from person to person due to disease, medical treatments, or genetic differences. The advantage of examining different sized segments from the same RNA species means that differences between individuals in transcription rates and/or stability should have little impact on the analysis since both segments will be present in approximately equimolar amounts at the time of death. As in this study, however, it would be prudent to avoid assaying clearly damaged or diseased teeth.

Further, our studies on bloodstains indicates that there are no significant differences in decay rates between the sexes, people of different ethnic backgrounds, or of different ages [15,28].

This preliminary study can be expanded to increase the accuracy of an estimate of PMI. Further experimental variables that the authors would like to pursue include analysis of the effect of temperature on the degradation of RNA in tooth pulp. This would include adding an accumulated degree day model to additional summer studies, along with corresponding studies in winter months. Another variable of interest, mentioned previously, is RNA degradation analysis of different types of RNA, including ribosomal RNAs (rRNAs). In previous studies presented by our laboratory to determine the time since deposition of bloodstains, we have shown that 18s rRNA is more stable than β-actin mRNA [15,16]. If these two species of RNA were to be used in combination in the detection of RNA degradation within postmortem tooth pulp, it is hypothesized that the span of time following death in which an estimate of PMI could be made would be greatly extended. Ultimately, these studies will need to be extended to teeth obtained from human corpses; ideally run in parallel with pig studies to determine the suitability of pigs as a model system for this means of estimating PMI in humans.

In conclusion, although this method of PMI estimation is in its early stages, we foresee several advantages over existing and previously proposed techniques. Unlike most other attempts to determine an extended PMI, the data presented here shows very little variation between pigs for any given *ex vivo* age. Additionally, the length of time over which estimates can be made (at least 84 days with our method *versus* roughly one month for most forensic entomology analyses) has been extended and estimates should be possible for specimens collected anywhere in the world. Entomological practices require knowledge of local insect fauna and species-specific growth curves as a function of temperature, which are not always available. The methods we employed are much more routine and widely available. Almost any competently trained molecular biologist could perform these genetic protocols, and the cost of reagents is under $100. Since teeth are as close to a closed system existing in mammals, the proposed method is not subject to environmental and other limitations to the degree of current estimators, factors such as fluctuations in humidity and consumption by scavengers. Additionally, the analysis can be completed in under a day. With further experimentation already underway, this technique shows promise to be an independent estimator of PMI that has the ability to greatly extend the time frame in which early estimates can be made.

Acknowledgements

We thank Dr. Barton Baker and the West Virginia University Davis College of Agriculture, Natural Resources & Design for the use of the field site on which these studies were conducted. We also thank all of our field volunteers for their efforts: Regina Trott, Tiffany Smith, Biatriz Vianna, Ashley Banks, Swati Banerjee, and Anne Perez. This project was supported by Awards No. 2003-RC-CX-K001 and 2010-DN-BX-K180, awarded by the National Institute of Justice, Office of Justice Programs, U.S. Department of Justice. The opinions, findings, and conclusions or recommendations expressed in this publication are those of the author(s) and do not necessarily reflect those of the Department of Justice. This research was also supported by an American Academy of Forensic Sciences' Lucas Grant.

References

[1] H. Gill-King, Chemical and ultrastructural aspects of decomposition, in: W.D. Haglund, M.H. Sorg (Eds.), Forensic Taphonomy: The Postmortem Fate of Human Remains, CRC Press, Boca Raton, 1997, pp. 93–104.
[2] T.D. Patten, A percentage method for representing the fall in body temperature after death. Its use in estimating the time of death. With a statement of theoretical basis of the percentage model, J. Forensic Med. 5 (1958) 2–15.
[3] M.A. Clark, M.B. Worrell, J.E. Pless, Postmortem changes in soft tissues, in: W.D. Haglund, M.H. Sorg (Eds.), Forensic Taphonomy: The Postmortem Fate of Human Remains, CRC Press, Boca Raton, 1997, pp. 151–160.
[4] A.A. Vass, S.A. Barshick, G. Sega, J. Caton, J.T. Skeen, J.C. Love, J.A. Synstelien, Decomposition chemistry of human remains: a new methodology for determining the postmortem interval, J. Forensic Sci. 47 (2002) 542–553.
[5] J.I. Coe, Postmortem chemistries on human vitreous humor, Am. J. Clin. Pathol. 51 (1969) 741–750.
[6] W.Q. Sturner, The vitreous humour: postmortem potassium changes, Lancet 1 (1963) 807–808.
[7] J.D. Wells, L.R. Lamotte, Estimating the postmortem interval, in: J.H. Byrd, J.L. Castner (Eds.), Forensic Entomology—The Utility of Arthropods in Legal Investigations, CRC Press, Boca Raton, 2010, pp. 367–388.
[8] R.D. Hall, N.H. Haskell, Forensic entomology—applications in medicolegal investigations, in: C. Wecht (Ed.), Forensic Sciences, Matthew Bender, New York, 1995.
[9] N.C. Collins, Developmental responses to food limitation as indicators of environmental conditions for *Ephydra cinerea* Jones (Diptera), Ecology 61 (1980) 650–661.
[10] R.W. Mann, W.M. Bass, L. Meadows, Time since death and decomposition of the human body: variables and observations in case and experimental field studies, J. Forensic Sci. 33 (1990) 102–111.
[11] C. Cattaneo, Forensic anthropology: developments of a classical discipline in the new millennium, Forensic Sci. Int. 165 (2007) 185–193.
[12] L.A. Benninger, D.O. Carter, S.L. Forbes, The biochemical alteration of soil beneath a decomposing carcass, Forensic Sci. Int. 180 (2008) 70–75.
[13] L.E. Van Belle, D.O. Carter, S.L. Forbes, Measurement of ninhydrin reactive nitrogen influx into gravesoil during aboveground and belowground carcass (*Sus domesticus*) decomposition, Forensic Sci. Int. 193 (2009) 37–41.
[14] Q. Liu, Q. Sun, Y. Liu, L. Zhou, N. Zheng, L. Liu, Bioluminescent assay of microbial ATP in postmortem tissues for the estimation of postmortem interval, J. Huazhong Univ. Sci. Technol. – Med. Sci. 29 (2009) 679–683.
[15] S. Anderson, B. Howard, G. Hobbs, C. Bishop, A method for determining the age of a bloodstain, Forensic Sci. Int. 148 (2005) 37–45.
[16] S. Anderson, G.R. Hobbs, C.P. Bishop, Multivariate analysis for estimating the age of a bloodstain, J. Forensic Sci. 56 (2011) 186–193.
[17] C. Hampson, J. Louhelainen, S. McColl, An RNA expression method for aging forensic hair sample, J. Forensic Sci. 56 (2011) 359–365.
[18] W.F. Libby, E.C. Anderson, J.R. Arnold, Age determination by radiocarbon content: world-wide assay of natural radiocarbon, Science 109 (1949) 227–228.
[19] H. Inoue, A. Kimura, T. Tuji, Degradation profile of mRNA in a dead rat body: basic semi-quantification study, Forensic Sci. Int. 130 (2002) 127–132.
[20] M. Bauer, I. Gramlich, S. Polzin, D. Patzelt, Quantification of mRNA degradation as possible indicator of postmortem interval—a pilot study, Leg. Med. 5 (2003) 220–227.
[21] D. Zhao, B.-L. Zhu, T. Ishikawa, L. Quan, H. Maeda, Real-time RT-PCR quantitative assays and postmortem degradation profiles of erythropoietin, vascular endothelial growth factor and hypoxia-inducible factor 1 alpha mRNA transcripts in forensic autopsy materials, Leg. Med. 8 (2006) 132–136.
[22] J.B. Duffy, M.F. Skinner, J.D. Waterfield, Rates of putrefaction of dental pulp in the northwest coast environment, J. Forensic Sci. 36 (1991) 1492–1502.
[23] L.M.L. Menon, K.F.B. Prado, R.H.A. da Silva, Histological evaluation of dentine and cementum after different periods of burial: an *in vitro* study, RSBO 8 (2) (2011) 131–137.
[24] Applied Biosystem's Guide to Performing Relative Quantitation of Gene Expression Using Real-Time Quantitative PCR, 2008. Part number 4371095 Revision B Life Technologies Corporation, Carlsbad, CA.
[25] Applied Biosystems, Real-time PCR: understanding CT, Application Note, 2008.
[26] K.J. Livak, T.D. Schmittgen, Analysis of relative gene expression data using real-time quantitative PCR and the $2^{-\Delta\Delta CT}$ method, Methods 25 (2001) 402–408.
[27] Adobe Systems Incorporated, RGB mode: specifying a color using numeric values, in: Adobe Photoshop 7.0 Help Manual, 2002.
[28] K.N. Nester, The use of β-actin mRNA degradation to estimate bloodstain age, Master's Thesis, Department of Biology, West Virginia University, USA, 2006, 56 pp.